

## Electronic supplementary information

### Multi-Scale Structured, Superhydrophobic and Wide-Angle, Antireflective Coating in the Near-Infrared Region

Kelly C. Camargo,<sup>†,\*</sup> Alexandre F. Michels,<sup>‡</sup> Fabiano S. Rodembusch,<sup>§</sup> and Flávio Horowitz,<sup>†</sup>

<sup>†</sup>Instituto de Física. Universidade Federal do Rio Grande do Sul, Porto Alegre, RS - Brazil

<sup>‡</sup>Centro de Ciências Exatas, da Natureza e de Tecnologia/UCS, Caxias do Sul, RS- Brazil

<sup>§</sup>Instituto de Química. Universidade Federal do Rio Grande do Sul, Porto Alegre, RS - Brazil

- **Wenzel regime.** Relates a roughness factor with the solid surface ( $r$ ), and the apparent contact angle of a liquid ( $\theta_c$ ) given by:

$$\cos \theta_c = r \cdot \cos \theta, r = (\text{Area})_{\text{real}} / (\text{Area})_{\text{projected}} \quad (1)$$

where  $\theta$  is the Young's contact angle that describes the contact angle on the plane smooth surface.

- **Cassie and Baxter regime.** An extension of Wenzel's equation to predict an increase of the apparent liquid contact angle when air is trapped between the liquid and the solid surfaces:

$$\cos \theta_c = f_1 \cdot \cos \theta - f_2, \quad (2)$$

where  $f_2$  is the liquid surface area fraction in contact with air. Equation (2) reduces to equation (1) when  $f_2$  is zero (with  $f_1 = r$ ). Wenzel's theory is applicable when the liquid completely fills the interstices on the solid surface which becomes hydrophilic. The Cassie-Baxter theory assumes that the liquid rests on top of the roughness features and thus on a composite air-solid surface.

#### References

- Marmur, A. *Langmuir* **2003**, *19*, 8343-8348.  
Plawsky, J. L.; Ojha, M.; Chatterjee, A.; Wayner Jr., P.C. *Chem. Eng. Comm.* **2008**, *196*, 658-696.

## EXPERIMENTAL

**Silica nanoparticles (SNPs).** All commercial solvents and reagents were used without further purification. Fumed silica nanoparticles (Aerosil® R972 - Degussa/Evonik), was used as received. The Aerosil® R972 is a hydrophobic fumed silica after treated with DDS (dimethyldichlorosilane) based on a hydrophilic fumed silica with a specific surface area of  $110\pm20\text{ m}^2/\text{g}$ , a carbon contend of 0.6-1.2 wt.% and an average primary particle size of 16 nm. The fumed silica nanoparticles were diluted in toluene to obtain a 1 wt% concentration.

**Silica aerogel.** Silica aerogel was prepared via sol-gel synthesis using tetraethoxysilane (TEOS) (Aldrich) as precursor following the procedure: TEOS hydrolysis in presence of ethanol 95% (Fluka) and deionized water under acidic conditions (HCl 0.1M Aldrich) at 60°C, with a molar ratio of  $1/3.8/1.1/7\times10^{-4}$  to TEOS/ethanol/H<sub>2</sub>O/HCl. After 90 min of stirring, aqueous ammonium hydroxide (Merck) was added with ethanol 95% at room temperature resulting in the final molar ratios  $1/38.8/3.6/7\times10^{-4}/2\times10^{-3}$  to TEOS/ethanol/H<sub>2</sub>O/HCl/NH<sub>4</sub>OH. Following gelation and ageing at 50°C, the gel was washed three times with ethanol and hexane. The aerogel in hexane was derivatized with trimethylchlorosilane (TMCS), and sonicated for 30 min to create a fluid sol suitable for dip coating.<sup>13-18</sup> Silica aerogel was deposited to produce a film, whose optical thickness corresponds to a quarter-wave layer in the near infrared region. After dip-coating, the film was dried for 2h at 250°C.

**WCA measurements.** Water contact angles (WCAs) were measured using the sessile drop method by deposition of 4-6 µL droplets of deionized water on horizontal dip-coated glass surfaces.<sup>24-27</sup> The droplets were observed directly in cross section with an Olympus BX-41 microscope objective lens, whereas their images were digitally captured using a 1.4 mega pixel computer-controlled digital CCD camera. The contact angle values were determined as averages over twenty measurements, performed in different areas of each sample surface. The sliding angle measurements were adjusted using a mechanical level goniometer. To determine hysteresis, advancing and receding contact angles were measured in both sides of the droplet, and in at least three different locations for each sample.

**Scanning Electron Microscopy (SEM) and Ellipsometry.** Film micro and nano-structures were characterized by Scanning Electron Microscopy (SEM). Thicknesses were measured by ellipsometry with spectral ellipsometer Sopra GES-5E.

**Transmittance.** Transmittances at various angles of incidence were measured with a Cary 5000 UV-VIS-IR spectrophotometer. A goniometer was attached on equipment to perform wide-angles measurements.

**PTFE-like layer monitoring.** The PTFE layer - with thicknesses of 200 nm and 55 nm in the two and three layer configurations, respectively - was deposited by time-controlled thermal physical vapor deposition (PVD) at room temperature, with a rate of 2.5 nm/min at  $10^{-5}$  Torr, and from a base pressure of  $2.10^{-6}$  Torr. A quartz microbalance monitor was used for thickness control. Furthermore the samples were characterized by Atomic Force Microscopy (AFM), which also was used for thickness post-deposition determination by comparison with a PTFE-free region, which had been masked previously to the PVD deposition. The obtained AFM results, which were not presented in this work, are in agreement with the thickness from the quartz microbalance.

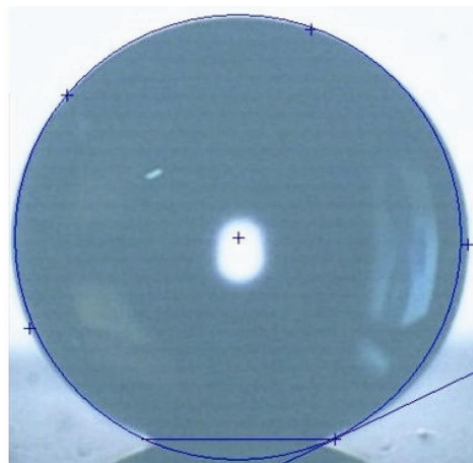


**Figure ESI1.** Droplet image with WCA angle of  $158^\circ \pm 2^\circ$  and less than  $5^\circ$  in angular hysteresis, from the second configuration based on silica nanoparticle clusters covered by silica aerogel and PTFE-like coating.

**Water drop test.** In the water drop test, about 1200 water droplets (ca. 90  $\mu\text{L}$ ) were dropped from about 35 cm above the sample. Afterwards the water contact angle was measured on the sample. The DI water contact angles were collected on samples before and after the tests.

## AFM pictures

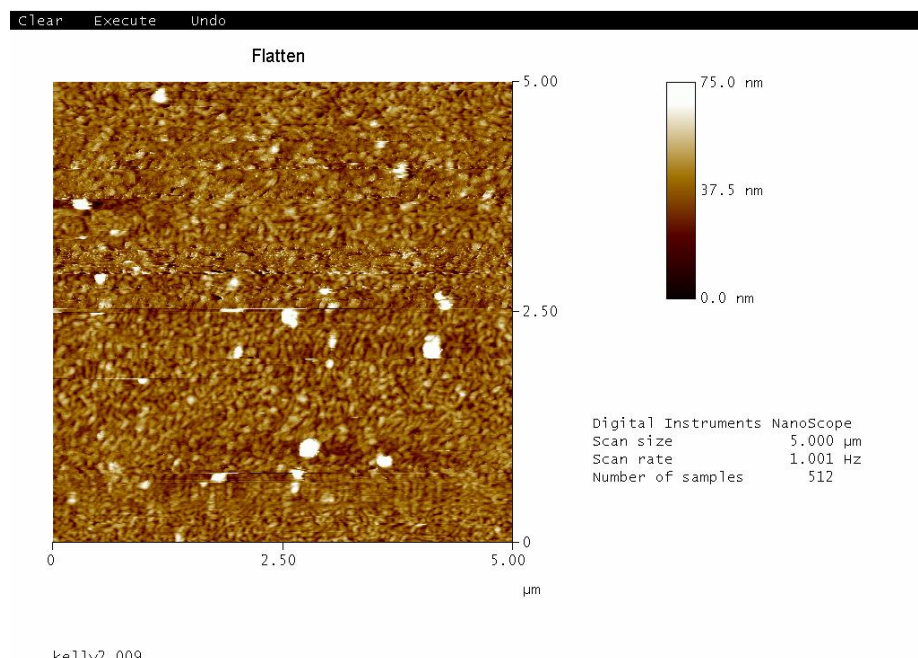


**Figure ESI2.** Two-layer configuration and roughness for PTFE-like layer.

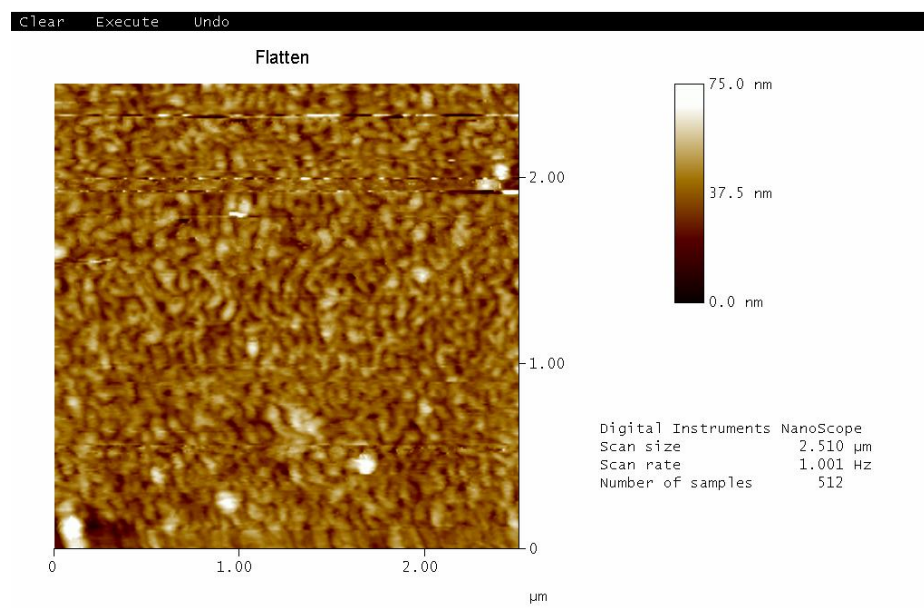


**Figure ESI3.** Two-layer configuration and roughness for PTFE-like layer.

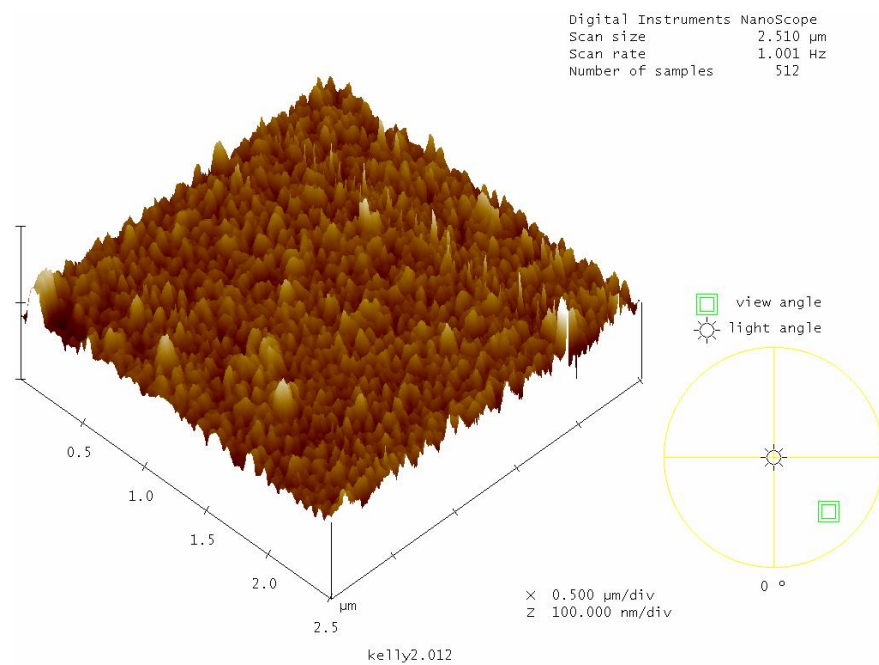


**Figure ESI4.** Two-layer configuration and roughness for PTFE-like layer.

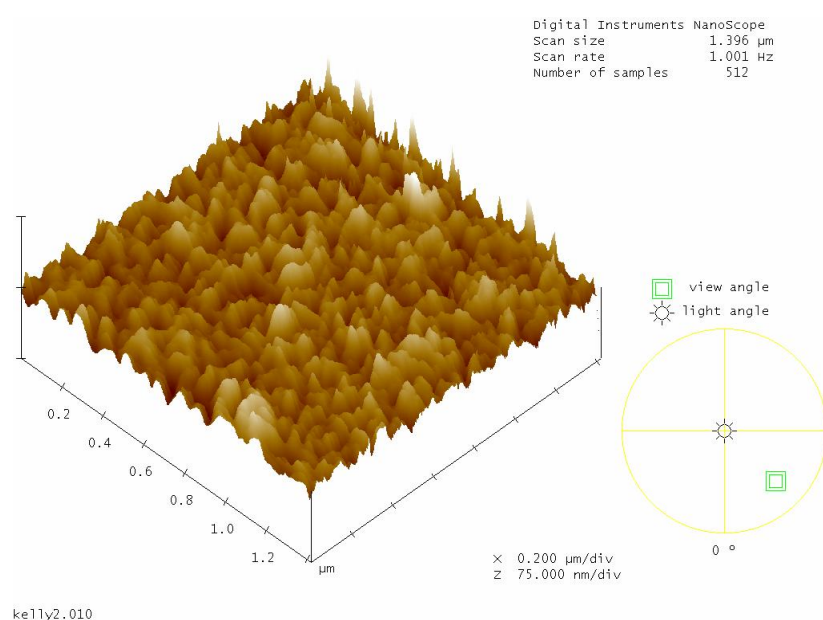


**Figure ESI5.** Two-layer configuration and roughness for PTFE-like layer.

**SEM pictures**

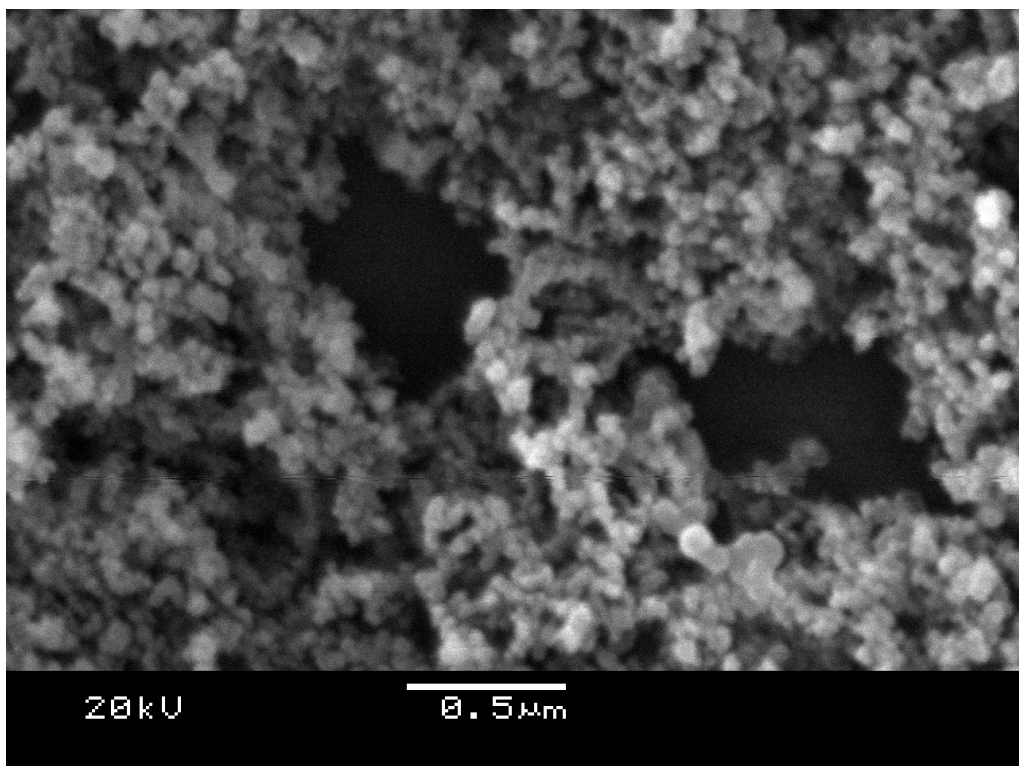


**Figure ESI6.** SEM pictures of the topology in the nanoscale level of the silica nanoparticles on the glass surface.

**Self-cleaning properties**



**Figure ESI7.** Sequence of self-cleaning properties of the obtained coatings.